Int. J. Electrochem. Sci., 16 **(2021)** Article ID: 210434, doi: 10.20964/2021.04.31

International Journal of
ELECTROCHEMICAL
SCIENCE
www.electrochemsci.org

Short Communication

Gold Nanoparticles Decorated on ZnONanorods/GCE for Enhanced Photocatalytic Degradation of Methylene Blue

Zhenzhen Jiang[1], *Junren Zhu*[2,*]

[1]Chongqing Vocational Institute of Engineering, Chongqing402260, P.R. China.
[2] Chongqing City Management College, Chongqing 401331, P.R. China.
[*]E-mail: zhujunren008@163.com

Received: 15 November 2020 / *Accepted:* 3 February 2021 / *Published:* 28 February 2021

Gold nanoparticles (Au NPs) decorated on ZnO nanorods (NRs) were synthesized via simple chemical bath deposition and thermal evaporation techniques on glassy carbon electrodes (GCE). The morphological, structural, photocatalyst and electrochemical properties of prepared samples were considered by FESEM, XRD, photodegradation and electrochemical analyses. FESEM results exhibited that high density and hexagonal wurtzite structure of Au NPs decorated on ZnO NRs were successfully synthesized on GCE substrate. The XRD analysis revealed the wurtzite structure of ZnO NRs and confirmed formation of Au NPs on ZnO NRs/GCE. The electrochemical studies indicated the specific capacitance enhancement of electric double-layer and conductivity improvement by Au NPs decorated on ZnO NRs. Photodegradation studies of methylene blue (MB) reveal that the degradation rate considerably was enhanced by Au NPs and the entire removal of MB was obtained after 60 min under sunlight irradiation. This considerable result can be related to the presence of Au NPs that reduced the recombination of photogenerated electron-hole pairs and the structural effect of one-dimensional ZnO NRs that enhance the light-harvesting ability. The photo-degradation kinetics and total percentage of photodegradation reveal that the photocatalytic activities of Au NPs-ZnO NRs/GCE was considerably higher with fast kinetic than that of ZnO NRs/GCE. It can be associated with a larger surface area of Au NPs-ZnO NRs compared to pure ZnO NRs.

Keywords: Gold nanoparticles; ZnOnanorods; Photocatalytic degradation; Methylene blue; Electrochemical analysis

1. INTRODUCTION

Degradation of hazardous and toxic molecules from wastewaters has attracted considerable attention [1, 2]. The photocatalytic method has been a promising technique to convert the pollutant to nontoxic molecules and remove the environmental pollution [3, 4]. Nanomaterials with new size-dependent characteristics show properties that are not indicated on the micro- or macroscale. They are hopeful tools for remediation and monitoring of wastewater polluted by microorganisms, heavy-metal

ions and organic/inorganic compounds. Photocatalytic reaction using semiconductors has appeared as a favorable wastewater treatment technique to overcome the main challenges created by conventional methods [5, 6]. So far, many semiconductor photocatalysts, such as WO_3, TiO_2, CuO, and ZnO have indicated promising photocatalytic activities, highlighting particularly ZnO due to its size-tunable physicochemical, lower cost and non-toxicity properties [7-10]. Nowadays, the key challenge for efficiency enhancement of the photocatalytic dye degradation by ZnO nanostructures is to prevent the photogenerated charge-carrier recombination (electron and holes) [11, 12]. Therefore, strategies like development of nanocomposites, doping, and nanostructuring have been approved to obtain this enhancement. Among the various types of nanostructures, one-dimensional nanostructures like nanowires and nanorods have received considerable attention because of their superior photocatalytic properties [13, 14]. Among the noble metallic nanoparticles (NPs), gold (Au) NPs has superior potential for decoration of ZnO nanorods and developing the photocatalytic activities [15]. Au NPs are reasonably soluble in water, optically sensitive, stable, and catalytically active. The unique optical property has enabled wide application of Au NPs as a SERS-active substrate [16, 17].

Methylene blue (MB) is one of the aromatic compounds of cyclic heterocycle in related and pharmaceutical industries [18-20]. This is an organic compound called the cationic dye thiazine which is used as an ultrasensitive redox oxidation electrochemical measurement due to its well-defined a redox-reaction at equilibrium. Moreover, there are numerous applications for MB dye as organic compounds due to relatively nontoxic, ready availability and low cost which lead to the increase of its water pollution [21].Therefore, removing these pollutants from contaminated water is imperative. However, many studies had been carried out to investigate degradation of MB in wastewater; obtaining high degradation efficiency is still a challenge among researchers. Thus, in this work, high density of Au NPs decorated ZnO nanorods on glassy carbon electrode (GCE) substrate were synthesized through chemical bath deposition and applied to consider as a superior degradation efficiency of the MB dyes.

2. MATERIALS AND METHODS

ZnO seed-layers were produced by a sol-gel technique on GCE substrates. First, GCE substrate was cleaned for 20 minutes in acetone, 20 minutes in ethanol, and then 20 minutes in DI water. All steps were done in an ultrasonic-bath. After that, the substrates were dried through a N_2 gas flux and 10 min UV-O3 exposure. For seed-layer production, a solution with a zinc acetate dihydrate (0.5 M) and monoethanolamine within a 1:1 molar ratio in ethanol solution was prepared. The mixture was transferred into an ultrasonic-bath at 50°C for 30 minutes and was maintained stirring at 50°C for an extra 30 minutes. Then, the precursor solutions were permitted to cool down to ambient temperature, and then, 250µL of solution was put on GCE through spin-coating at 3000 rpm for 20 s. Finally, the films were annealed by a hot plate at 400°C for 10 min in air.

ZnO nanorods were prepared by chemical bath deposition (CBD). A prepared solution including 30 mM hexamethylenetetramine and 30 mM zinc nitrate hexahydrate were mixed in DI water. Ultrasonication was done for 10 min at room temperature. After that, the prepared solution was stirred onto hot-plate at ambient temperature for 20 minutes. ZnO nanorods were grown at 70°C for 60

minutes. A 30 mL solution was utilized for each substrate. Then the specimens were cleaned using DI-water and dried by N_2. To prepare the Au NPs decorated on ZnO nanorods, a thin-layer of Au NPs were deposited on ZnO nanorods by thermal evaporation technique in the vacuum chamber in 1×10^{-6}mbar with a deposition rate of 0.2 Å/s.

The morphology of prepared samples was considered by scanning electron microscopy (SEM). The X-ray diffractometer with Cu Kα radiation at wavelength of 1.5404Å operating at 30 kV and 20 mA was used to investigate the crystal structures of specimens.CV and EIS measurements were performed with Metrohm Auto lab instruments in a standard three-electrode electrochemical cell which contained Ag/AgCl electrode as a reference electrode, Pt wire as a counter electrode and the prepared pure ZnO and Au NPs/ZnO NRs as working electrode. The electrolyte of CV measurements was 0.1 M phosphate buffer solutions (PBS) with pH 6. The CV characterization was done at 10 mVs^{-1}scan rate with potential ranges from 0.0 to 0.3 V. The electrolyte solution of EIS experiments was 0.5 M Na_2SO_4 (99%, Tianjin Wodehaotai Trading Co., Ltd., China). The EIS analysis was performed at frequency range of 0.1 Hz to 0.1 MHz at 5 mV applied voltage. The degradation activity of all the samples were performed for MB (10 mgl^{-1}) under sunlight irradiation. The UV/Vis spectrophotometer (UV-2100, China) was used to measure the absorbance spectra of the MB solution.

3. RESULTS AND DISCUSSION

Figure 1 indicates the morphology of prepared ZnO nanorods and Au NPs/ZnO NRs on GCE substrate. The pure ZnO NRs have uniform morphologies and are dense with average diameter of 150 nm and length of about 900 nm with a growth c-axis along the [0001] direction. Furthermore, Au NPs with diameters from 15 nm to 20 nm were homogeneously distributed onto the ZnO NRs/GCE.

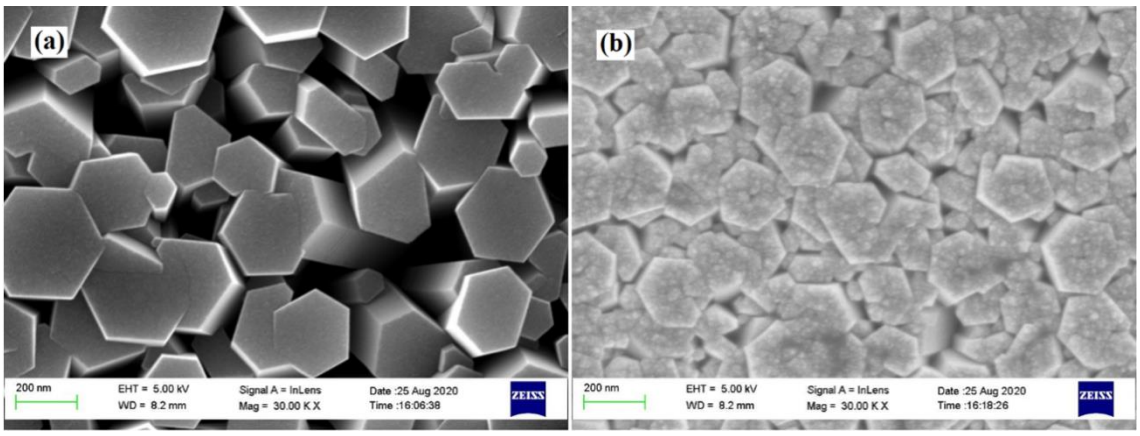

Figure 1. FESEM images of (a) pure ZnO NRs and (b) Au NPs/ZnO NRs on GCE substrate

XRD patterns of ZnO NRs and Au NPs decorated on ZnO NRs are shown in Figure 2. The peaks at 2θ= 31.7°, 34.3°, 36.3°, 47.6°, 56.7°, 62.8°, 66.5°, 67.9°, and 69.2° are found which

correspond to (100), (002), (101), (102), (110), (103), (200), (112), and (201) planes of ZnO, respectively [22, 23]. It shows that ZnO nanostructures crystallize in a hexagonal (wurtzite) crystal structure (JCPDS, card No. 36-1451). Extra diffraction peaks were observed in comparison with pure ZnO NRs at the location of 2θ= 38.3°, 44.5°, 64.8°, 77.7° which attributed to the (111), (200), (220), and (311) planes of face-centered cubic Au (JCPDS card 04-0784) [24], which is compatible with SEM results.

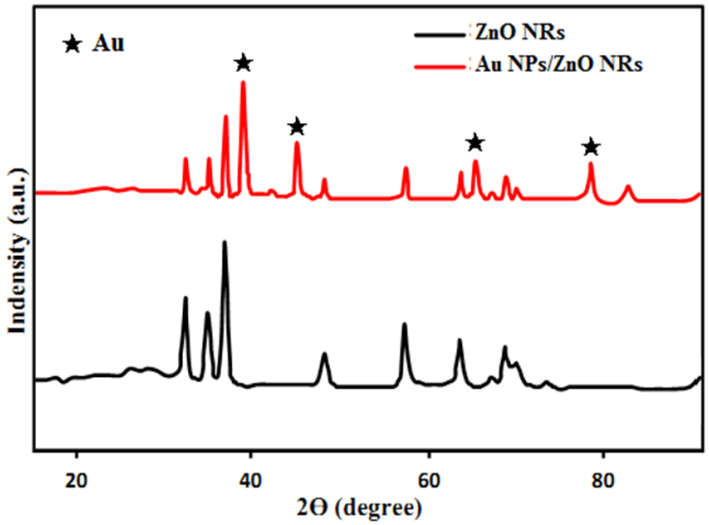

Figure 2. XRD pattern of pure ZnO nanorods and Au NPs-ZnO nanorods deposited on GCE substrates

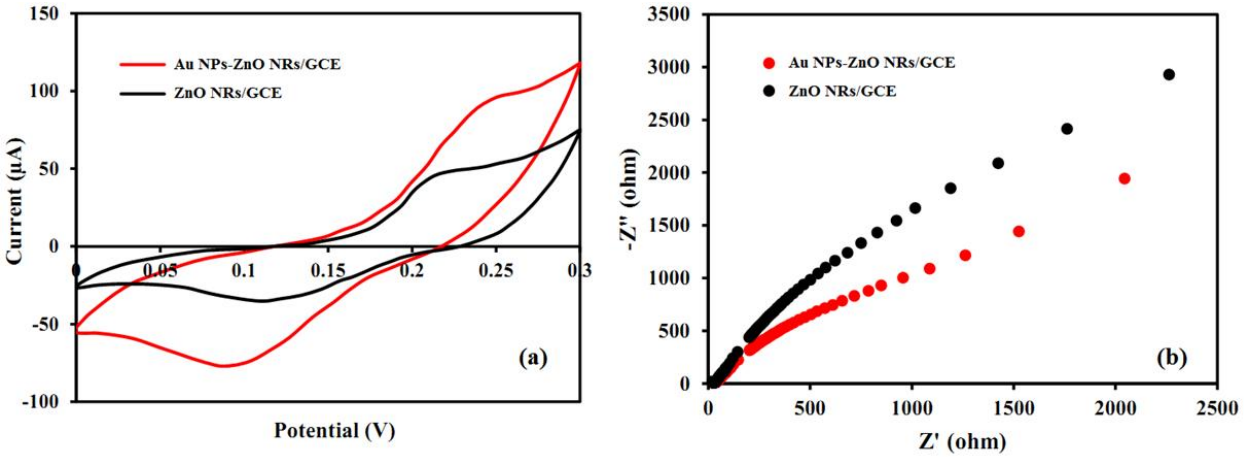

Figure 3. (a)CV plots of ZnO NRs/GCE and Au NPs-ZnO NRs/GCE in 0.1 M PBS (pH 6) solution at 10 mVs^{-1}scan rate with potential ranges between 0 to 0.3 V (b) The Nyquist diagrams of ZnO NRs/GCE and Au NPs-ZnO NRs/GCE with frequency range of 0.1 Hz to 0.1 MHz at 5 mV applied voltage into Na_2SO_4 solution (0.5 M)

Figure 3a indicates the CV results of pure ZnO NRs and Au NPs-ZnO NRs on GCE in 0.1 M PBS (pH 6) solution at 10 mVs^{-1}scan rate with potential ranges between -0.1 to 0.8 V. As indicated in Fig. 3a, Au NPs-ZnO NRs/GCE reveals greater surrounding area of recorded CV than the ZnO

NRs/GCE sample which shows the specific capacitance improvement of electric double-layer due to the Au NPs onto the ZnO structures [25]. It can improve the charge-storage value and superior electronic-storage capability of Au NPs-ZnO NRs toward pure ZnO NRs. EIS assessments were done to consider samples in frequency range of 0.1 Hz to 0.1 MHz at 5 mV applied voltage into Na_2SO_4 solution (0.5 M). Figure 3b indicates the Nyquist diagrams of the specimens that was clearly exhibited smaller resistance of Au NPs-ZnO than undecorated ZnO NRs, which related to enhancement of the conductivity of ZnO NRs by coating Au NPs on ZnO nanostructures because of the synergistic effect between Au and ZnO nanorods [26]. Moreover, high electron-transfer rate can be associated with more interfaces between Au and ZnO [27].

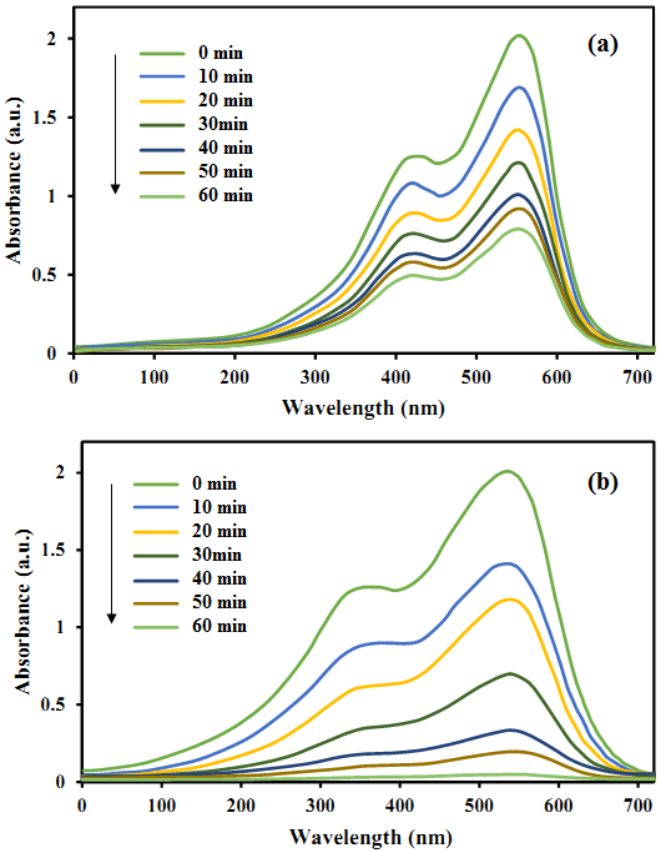

Figure 4. Photocatalytic activity of (a) ZnO NRs/GCE and (b) Au NPs-ZnO/GCE in degradation of 10 mgl^{-1}MB dye under sunlight irradiation

The photocatalytic activities of ZnO NRs/GCE and Au NPs-ZnO NRs/GCE were assessed based on the efficiency of photodegradation for MB dye under sunlight irradiation. To study the efficiency of prepared samples for the MB degradation, each electrode was considered under the same condition as a function of the irradiation time. These results are indicated in Figure 4, which shows the UV-visible spectra of MB dye recorded at various time intervals in the photodegradation tests. The photodegradation percentages were calculated using eq 1 [28].

$$\%\ degradation = \frac{(C0-C)}{C0} \times 100 \qquad (1)$$

where C represents the concentration of MB dye after degradation and C_0 indicates initial concentration of MB dye. The degradation percentage of ZnO NRs/GCE after sunlight irradiation for 60 min was around 61%. As shown in figure 4b, a superior activity was obtained by the Au NPs-ZnO NRs/GCE with about 100% photodegradation of MB dye after sunlight irradiation for 60 min. This considerable result can be related to the presence of Au NPs that reduced the recombination of photogenerated electron-hole pairs and the structural effect of one-dimensional ZnO NRs that enhance the light-harvesting ability, which significantly promoted photoactivity of the catalysts [29]. The increase of hydroxyl radicals produced by catalysts was influenced through synergistic effect of the Au NPs on the activity of ZnO NRs by electron-hole trapping [30].

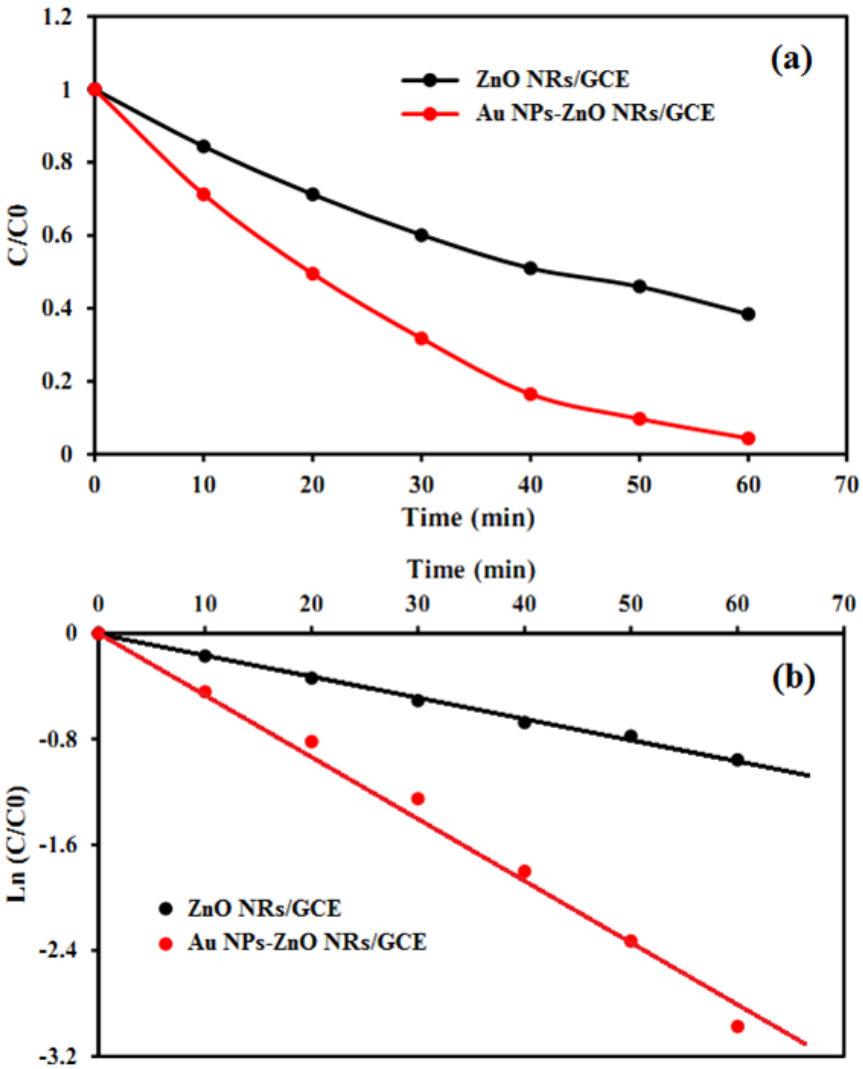

Figure 5. Kinetic diagrams of the photodegradation reactions of 10 mgl^{-1}MB dye in the presence of ZnO NRs/GCE and Au NPs-ZnO NRs/GCEunder sunlight irradiation

The photocatalytic mechanism of Au NPs-ZnO NRs is suggested as follows. The ZnO nanostructures act as hole and electron sources. The electron-hole pair of zinc oxide nanostructures are produced by UV excitation [31]. The electrons in the conduction-band are relaxed to the level of the defect and then reacted by the electron acceptors in oxygen to form oxygen ion superoxide, and valence-band holes react with H_2O to create hydroxide ion (OH^-) [32]. The photocatalytic activities are mostly related to the oxygen amount [33]. But the essential electrons for creation of O_2 may be lost by electron-hole pair recombination. Au nanoparticles act as electron sinks to trap photogenerated electrons from the semiconductors and lead to the shift Fermi-level to more negative potential [34]. The Au NPs-ZnO NRs interface may move electrons from zinc oxide nanostructures to gold nanoparticles through a charge equilibration procedure and lower electron-hole pair recombination to improve photocatalytic activities [35]. Furthermore, the work function of ZnO is smaller than that of the Au, and therefore, a Schottky barrier forms at a junction which leads to inhibiting electron injection and enabling the electron capture.

The photodegradation reaction for MB dye follows pseudo-first-order reaction kinetics and the reaction rate constant (k) is assessed by the following equation, where t shows the sunlight irradiation time [36].

$$\text{Ln } C/C0 = -kt \qquad (2)$$

Table 1. Comparison of degradation efficiency of MB on Au NPs-ZnO NRs surface with other nanostructured photocatalysts

Photocatalysts	**MB concentration (mg l^{-1})**	**Time (minutes)**	**Degradation efficiency (%)**	**Ref**
Fe-doped ZnO nanoparticles	20	120	58	[37]
ZnO/graphene	10	40	94	[38]
Al/Fe co-doped ZnO NRs	10	75	94	[39]
ZnO nanoparticles	20	240	100	[40]
Ag-ZnO nanostructures	10	60	98	[41]
Au NPs-ZnO NRs	10	60	100	This work

Figure 5 indicates kinetic diagrams of the photodegradation reactions of MB dye in the presence of ZnO NRs/GCE and Au NPs-ZnO NRs/GCE. The degradation of MB dye by the Au NPs-ZnO NRs/GCE photocatalyst indicated fastest kinetics with a reaction rate constant of 0.0464 min^{-1}, which was more than 3 times of the reaction rate constant (0.0159 min^{-1}) for degradation of MB dye by the ZnO NRs/GCE photocatalyst.The photo-degradation kinetics and total percentage of photodegradation reveal that the photocatalytic activities of Au NPs-ZnO NRs/GCE was considerably higher with fast kinetic than that of ZnO NRs/GCE. It can be associated with larger surface area of Au

NPs-ZnO sample compared to pure ZnONRs.Moreover, the improved photocatalytic activity of Au NPs-ZnO NRs can be related to its porous-like structure, which may enhance the trapping and adsorption of the MB dye inside the nanorod arrays, as confirmed by the FESEM images.

Comparison the photodegradation efficiency of MB on Au NPs-ZnO NRs surface with other nanostructured photocatalysts is presented in Table 1. As seen, by considering the time of photodegradation, Au NPs-ZnO NRs show the degradation efficiency of 100% for 60 min, which are higher than the reported degradation efficiency values in[37-41].

4. CONCLUSIONS

Au NPs decorated on ZnO NRs were synthesized via simple CBD and thermal evaporation techniques on GCE. The morphological, structural, photocatalyst and electrochemical properties of prepared samples were considered by FESEM, XRD, photodegradation and electrochemical analyses. FESEM results exhibited that high density and hexagonal wurtzite structure of Au NPs decorated on ZnO nanostructures were successfully synthesized on GCE substrate. XRD results show hexagonal (wurtzite) crystal structure of ZnO and face-centered cubic structure of Au, which is compatible with SEM results. The electrochemical studies indicated the specific capacitance enhancement of electric double-layer and conductivity improvement by Au NPs decorated on ZnO NRs. Photodegradation studies of methylene blue (MB) reveal that the degradation rate considerably was enhanced by Au NPs and the entire removal of MB was obtained after 60 min under sunlight irradiation. This considerable result can be related to the presence of Au NPs that reduced the recombination of photogenerated electron-hole pairs and the structural effect of one-dimensional ZnO NRs that enhance the light-harvesting ability. The photo-degradation kinetics and total percentage of photodegradation reveal that the photocatalytic activities of Au NPs-ZnO NRs/GCE was considerably higher with fast kinetic than that of ZnO NRs/GCE.The improved photocatalytic activity of Au NPs-ZnO NRs can be related to its porous-like structure, which may enhance the trapping and adsorption of the MB dye inside the nanorod arrays, as confirmed by the FESEM images.

ACKNOWLEDGEMENT
The authors are grateful for the financial support provided by the Scientific and Science and Technology Research Program of Chongqing Municipal Education Commission (Grant No.KJQN202003306, No.KJQN201903408 and No.KJQN201803307), and Natural Science Foundation of Chongqing (Grant No.cstc2020jcyj-msxmX0949).

References

1. P. Sirajudheen, P. Karthikeyan, S. Vigneshwaran, M. Nikitha, C.A. Hassan and S. Meenakshi, *Carbohydrate Polymer Technologies and Applications*, 1 (2020) 100018.
2. H. Karimi-Maleh, M. Alizadeh, Y. Orooji, F. Karimi, M. Baghayeri, J. Rouhi, S. Tajik, H. Beitollahi, S. Agarwal and V.K. Gupta, *Industrial & Engineering Chemistry Research*, 60 (2021) 816.

3. N.S. Alharbi, B. Hu, T. Hayat, S.O. Rabah, A. Alsaedi, L. Zhuang and X. Wang, *Frontiers of Chemical Science and Engineering*, 14 (2020) 1.
4. S. Tang, Z. Wang, D. Yuan, Y. Zhang, J. Qi, Y. Rao, G. Lu, B. Li, K. Wang and K. Yin, *International Journal of Electrochemical Science*, 15 (2020) 2470.
5. N. Yahya, F. Aziz, N. Jamaludin, M. Mutalib, A. Ismail, W. Salleh, J. Jaafar, N. Yusof and N. Ludin, *Journal of environmental chemical engineering*, 6 (2018) 7411.
6. R. Bashiri, N.M. Mohamed, C.F. Kait, S. Sufian, S. Kakooei, M. Khatani and Z. Gholami, *Renewable Energy*, 99 (2016) 960.
7. Y. Lu, R. Jin, Y. Qiao, W. Liu, K. Wang, X. Wang and C. Wang, *International Journal of Electrochemical Science*, 15 (2020) 10243.
8. M.B. Tahir, G. Nabi and N. Khalid, *Materials Science in Semiconductor Processing*, 84 (2018) 36.
9. H. Karimi-Maleh, S. Ranjbari, B. Tanhaei, A. Ayati, Y. Orooji, M. Alizadeh, F. Karimi, S. Salmanpour, J. Rouhi and M. Sillanpää, *Environmental Research*, 195 (2021) 110809.
10. R. Mohamed, J. Rouhi, M.F. Malek and A.S. Ismail, *International Journal of Electrochemical Science*, 11 (2016) 2197.
11. K. Chaudhary, N. Shaheen, S. Zulfiqar, M.I. Sarwar, M. Suleman, P.O. Agboola, I. Shakir and M.F. Warsi, *Synthetic Metals*, 269 (2020) 116526.
12. F. Zhang, W. Zhang, X. Luo, G. Feng and L. Zhao, *International Journal of Electrochemical Science*, 12 (2017) 3756.
13. J. Xiong, Y. Gan, J. Zhu, W. Li, C. Gao, Y. Wei, G. Cheng, Z. Li and S. Dou, *Inorganic Chemistry Frontiers*, 4 (2017) 2075.
14. M. Alimanesh, J. Rouhi and Z. Hassan, *Ceramics International*, 42 (2016) 5136.
15. A. Abdal Dayem, S.B. Lee and S.-G. Cho, *Nanomaterials*, 8 (2018)
16. B.R. Gangapuram, R. Bandi, M. Alle, R. Dadigala, G.M. Kotu and V. Guttena, *Journal of Molecular Structure*, 1167 (2018) 305.
17. H. Karimi-Maleh, Y. Orooji, A. Ayati, S. Qanbari, B. Tanhaei, F. Karimi, M. Alizadeh, J. Rouhi, L. Fu and M. Sillanpää, *Journal of Molecular Liquids*, (2020) 115062.
18. G. Sharma, A. Kumar, S. Sharma, M. Naushad, T. Ahamad, S.I. Al-Saeedi, G.M. Al-Senani, N.S. Al-Kadhi and F.J. Stadler, *Journal of Molecular Liquids*, 272 (2018) 170.
19. N.M. Mohamed, R. Bashiri, F.K. Chong, S. Sufian and S. Kakooei, *international journal of hydrogen energy*, 40 (2015) 14031.
20. J. Rouhi, S. Kakooei, S.M. Sadeghzadeh, O. Rouhi and R. Karimzadeh, *Journal of Solid State Electrochemistry*, 24 (2020) 1599.
21. B. Wang, B. Dong, M. Xu, C. Chi and C. Wang, *Chemical Engineering Science*, 168 (2017) 90.
22. G. Sathishkumar, C. Rajkuberan, K. Manikandan, S. Prabukumar, J. DanielJohn and S. Sivaramakrishnan, *Materials Letters*, 188 (2017) 383.
23. K. Eswar, J. Rouhi, H. Husairi, M. Rusop and S. Abdullah, *Advances in Materials Science and Engineering*, 2014 (2014) 1.
24. A.I. Usman, A.A. Aziz and O.A. Noqta, *Materials Today: Proceedings*, 7 (2019) 803.
25. S. Najib, F. Bakan, N. Abdullayeva, R. Bahariqushchi, S. Kasap, G. Franzò, M. Sankir, N.D. Sankir, S. Mirabella and E. Erdem, *Nanoscale*, 12 (2020) 16162.
26. H.Q. Huynh, K.N. Pham, B.T. Phan, C.K. Tran, H. Lee and V.Q. Dang, *Journal of Photochemistry and Photobiology A: Chemistry*, 15 (2020) 112639.
27. G. Wu, G. Zhao, J. Sun, X. Cao, Y. He, J. Feng and D. Li, *Journal of catalysis*, 377 (2019) 271.
28. Y. Hunge, A. Yadav and V. Mathe, *Journal of Materials Science: Materials in Electronics*, 29 (2018) 6183.
29. H. Moussa, E. Girot, K. Mozet, H. Alem, G. Medjahdi and R. Schneider, *Applied Catalysis B: Environmental*, 185 (2016) 11.

30. R.M. Kakhki, R. Tayebee and F. Ahsani, *Journal of Materials Science: Materials in Electronics*, 28 (2017) 5941.
31. K. Rahimi, A. Yazdani and M. Ahmadirad, *Materials & Design*, 140 (2018) 222.
32. H.-F. Lin, S.-C. Liao and S.-W. Hung, *Journal of Photochemistry and Photobiology A: Chemistry*, 174 (2005) 82.
33. Y. Li, Y. Li, X. Xu, C. Ding, N. Chen, H. Ding and A. Lu, *Chemical Geology*, 504 (2019) 276.
34. L. Shi, Z. Li, K. Marcus, G. Wang, K. Liang, W. Niu and Y. Yang, *Chemical Communications*, 54 (2018) 3747.
35. S. Faraji, S.A. Ghasemi, S. Rostami, R. Rasoulkhani, B. Schaefer, S. Goedecker and M. Amsler, *Physical Review B*, 95 (2017) 104105.
36. S. Raj, H. Singh, R. Trivedi and V. Soni, *Scientific Reports*, 10 (2020) 1.
37. R. Saleh and N.F. Djaja, *Superlattices and Microstructures*, 74 (2014) 217.
38. T. Xu, L. Zhang, H. Cheng and Y. Zhu, *Applied Catalysis B: Environmental*, 101 (2011) 382.
39. N. Khalid, A. Hammad, M. Tahir, M. Rafique, T. Iqbal, G. Nabi and M. Hussain, *Ceramics International*, 45 (2019) 21430.
40. I. Kazeminezhad and A. Sadollahkhani, *Journal of Materials Science: Materials in Electronics*, 27 (2016) 4206.
41. S.S. Patil, M.G. Mali, M.S. Tamboli, D.R. Patil, M.V. Kulkarni, H. Yoon, H. Kim, S.S. Al-Deyab, S.S. Yoon and S.S. Kolekar, *Catalysis Today*, 260 (2016) 126.